

QUALITY AND RELIABILITY ASSURANCE RESEARCH AT MSFC

September 29, 1966

By

James B. Beal  
Robert L. Brown  
Leon C. Hamiter, Jr.  
Frederic E. Wells



# FAST SCAN INFRARED MICROSCOPE FOR IMPROVING MICROELECTRONIC DEVICE RELIABILITY

by Leon C. Hamiter, Jr.

	Page
SUMMARY. . . . .	1
INTRODUCTION. . . . .	1
INFRARED RADIATION. . . . .	1
INFRARED MICROSCOPE. . . . .	2
FUTURE PLANS. . . . .	5

## LIST OF ILLUSTRATIONS

Figure		Page
1.	List of Semiconductor Defects. . . . .	1
2.	Fast Scan Infrared Microscope. . . . .	2
3.	Block Diagram of Fast Scan Infrared Microscope. . . . .	3
4.	Schematic Diagram and Physical Layout of Dual Gate. . . . .	4
5.	Fifty Infrared Scan Lines of Microcircuit. . . . .	4
6.	Infrared Profile and Photograph of Microcircuit. . . . .	5
7.	Single Scan IR Superimposed on Circuit Schematic. . . . .	5
8.	IR Scan of Circuit at 0, 1, 6, 16, 46 Seconds During Warmup as Related to X-Ray of Unit. . . . .	6
9.	IR Scan of Circuit With a Crack in the Silicon. . . . .	6
10.	Power Transistor Used for Second Breakdown Study . . . . .	6
11.	Normal and Second Breakdown Infrared Emission. . . . .	7
12.	Area Where Second Breakdown Occurred . . . . .	7

## USE OF SLURRIES FOR HYDROSTATIC TESTING

by Frederic E. Wells

	Page
SUMMARY. . . . .	9
INTRODUCTION. . . . .	9
CRITERIA FOR SLURRIES. . . . .	9
GEORGIA INSTITUTE OF TECHNOLOGY STUDY. . . . .	10
PERFORMANCE TESTS ON LEAD OXIDE AND BARIUM SULFATE SLURRIES. . . . .	10
ECONOMIC CONSIDERATIONS. . . . .	11
FUTURE PLANS. . . . .	11

## AUTOMATED ULTRASONIC SCANNING BY TRIANGULATION METHODS - THE DICKINSON SYSTEM

by Robert L. Brown

	Page
SUMMARY. . . . .	13
INTRODUCTION. . . . .	13
ACOUSTIC SPECTROMETER. . . . .	13

### LIST OF ILLUSTRATIONS

Figure		Page
1.	Acoustic Spectrometer Inspection of S-IC Fuel Tank Section. . . . .	14
2.	Location of Flaws by Multiple Wave Directors. . . . .	15
3.	Block Diagram of Acoustic Spectrometer System. . . . .	16

# ULTRASONIC EMISSION DETECTOR EVALUATION OF THE STRENGTH OF BONDED MATERIALS

by James B. Beal

	Page
SUMMARY. . . . .	19
INTRODUCTION. . . . .	19
ADHESIVE BONDING. . . . .	20
EVALUATION OF ADHESIVE BOND STRENGTH. . . . .	20
ULTRASONIC EMISSION DETECTOR. . . . .	22
CONCLUSION. . . . .	26
REFERENCES. . . . .	27
BIBLIOGRAPHY. . . . .	27

## LIST OF TABLES

Table		Page
I.	Reduction of Bonding Problems by Using Nondestructive Testing. . . . .	19
II.	Bond Strength Prediction Results. . . . .	25

## LIST OF ILLUSTRATIONS

Figure		Page
1.	Photomicroflaw Techniques. . . . .	21
2.	Photomicroflaw Control of Bond Strength with Lap Shear Samples. . . . .	21
3.	Flatwise Ring Tension Test Apparatus. . . . .	22
4.	Ultrasonic Emission Detector Apparatus. . . . .	23
5.	Block Diagram of Ultrasonic Emission Detector. . . . .	23
6.	Stress Noise Emission Spectrum for HT-424 Adhesive in Flatwise Tension and 40% Bondline Contamination. . . . .	24



# FAST SCAN INFRARED MICROSCOPE FOR IMPROVING MICROELECTRONIC DEVICE RELIABILITY

By

Leon C. Hamiter, Jr.

## SUMMARY

The emission of infrared radiation by semiconductor chips led to a method for testing micro-miniature circuits with an infrared microscope. A description of infrared radiation is presented and is related to the electrical power dissipation of an electronic part. A description of the composition and operation of the infrared microscope is presented. The feasibility of inspection of the elements and circuit junctions of microelectronic chips is demonstrated. Thermal maps of circuits are examined for defects and design problems. The possibility of using the infrared microscope for testing transistors is discussed.

## INTRODUCTION

Technological progress is a two-step function. First, a new device is created, and second, means to manufacture it in a better and more consistent way are sought. The world of microelectronics is now in the second phase, with progress being made towards better manufacturing methods and processes.

Infrared testing is being developed to yield large amounts of information on thermal and electromechanical parameters affecting the reliability of microelectronic devices. Conventional test equipment and methods cannot measure these factors because of the minute size and inaccessibility of the elements.

Semiconductor chips have an area approximately  $1 \text{ mm}^2$ , and within this chip some integrated circuits contain dozens of transistors, diodes and resistors. The electrical interconnections are often only a few microns in width, which makes physical contact with them for test purposes not only difficult but also dangerous to their mechanical and electrical integrity. On a practical basis, probe measurements can only be made prior to dicing and encapsulation.

Ordinarily, only input and output measurements can be obtained through the use of conventional test equipment. In the case of complex integrated circuitry this is inadequate because it does not give information about the performance of the individual elements of the network. Marginal performance of an element could go undetected because of the compensating effect of another element. Furthermore, several design or manufacturing defects that may eventually cause a failure cannot be detected by conventional testing. Figure 1 shows some of the failure mechanisms and defective conditions in this class.

SEMICONDUCTOR BULK MATERIAL	RESISTIVITY IRREGULARITIES DISLOCATIONS LATTICE ANOMALIES SECONDARY BREAKDOWN
DESIGN	JUNCTION PROXIMITY THERMAL INTERACTION
SURFACE	PINHOLES CONTAMINATION ION MIGRATION CHANNELING
MECHANICAL	UNEVEN METAL DEPOSITION POOR BONDING OF DEPOSITED ELEMENTS POOR BONDING OF LEAD WIRES POOR DIE BONDING CRACKS, VOIDS, AND SCRATCHES

FIGURE 1. LIST OF SEMICONDUCTOR DEFECTS

## INFRARED RADIATION

Infrared radiation, or "invisible light," is an electromagnetic oscillation of the same type as the electromagnetic waves that are called "visible light." The electromagnetic radiation band extends from the very low frequencies of the typical house current oscillations to the extremely high frequencies of the gamma rays and cosmic rays produced by variations in energy of subatomic particles. All of these radiations are of the same nature, travel at the same speed (the speed of light), and transport energy.

The infrared radiation is contained in the band between the visible light and the radio waves. The infrared radiation is generated by the vibrational and rotational movements of the atoms and the molecules of which physical matter is composed. Consequently, the spectrum of the infrared radiation emitted by physical matter is extremely broad and peaks at a frequency that varies with temperature.

A physical body containing atomic and subatomic particles of all possible sizes would emit at all infrared frequencies, on an uninterrupted spectral band. Such a physical body is called a "blackbody," and although it does not exist in nature, very close approximations to it can be made, and infrared radiation laws are formulated upon it. The shape of this component's radiation band will depend upon its temperature and surface condition, or "emissivity."

Besides the infrared radiation emitted by physical matter because of thermal agitation, infrared radiation is also being emitted by semiconductors independently from the thermal status. This infrared radiation is called recombination radiation and results from the energy liberated by the current carriers when they step down from the higher energy level of the carrier band to the lower energy level of the valence band (the electron hole pairs recombine). This recombination radiation is directly proportional to the amount of current flowing through the semiconductor and its variations of the current flow. Detection and measurement of the recombination radiation should allow the modulated operation and even pulse operation of semiconductors to be analyzed without any time delay. The recombination radiation takes place in a different wavelength than the radiation caused by thermal effects, and with the use of adequate filters, each radiation can be read independently.

Wherever electrical current flows, a fraction of it turns into heat. This is generally called "power dissipation" and results in a temperature rise of the element through which the current flows. This thermal rise increases the power of the infrared radiation emitted by the surface of the element, and in turn this variation can be measured by an adequate infrared detector.

A direct correlation can be established between the electrical power dissipation of an electronic part of a given design, and the infrared radiation emitted by it. This correlation is the key to the infrared evaluation of electrically energized micro-electronic circuits.

Passive elements can be evaluated by plotting their temperature variation when subjected to a thermal gradient. This is done by mapping the infrared radiation emitted by each surface point of the target. Then the physical anomalies such as material discontinuities, lack of proper bonding, cross-section variations, etc., can be detected and evaluated.

When the target is a semiconductor chip, the infrared test equipment requirements are set by its physical size, the temperature gradients to be observed and the speed at which thermal flooding of the target takes place.

## INFRARED MICROSCOPE

Figure 2 is a photograph of the fast scan infrared microscope developed by Raytheon Company under contract for MSFC. On the left is the pedestal for mounting the device under examination. The microscope is for alignment and visual observation of the sample. The upper right area contains the drive mechanism for the helix and polygon scanning system. Figure 3 is a functional block diagram of the instrument. Basically the unit can be divided into five major sections: optics, scanning system, detector with cryogenic cooling, signal processing and display system.

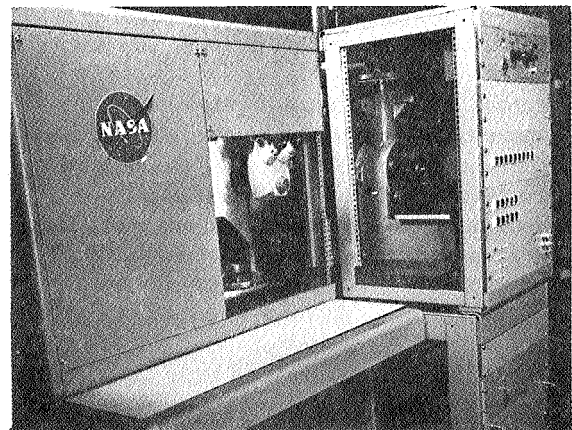


FIGURE 2. FAST SCAN INFRARED MICROSCOPE

### OPTICS

Larger than normal optics with several unique properties were deliberately chosen for the infrared microscope. The detector aperture requirements were satisfied by using a 7.6 to 1 magnifying system.

DETECTOR WITH CRYOGENIC COOLING

The detector and the cooling system were chosen to be compatible with the rest of the microscope. The detector has a 0.000762-centimeter (0.0003-inch) diameter aperture with an aperture limiting mask of 13 degrees in one axis and 6 degrees in the other axis. This aperture will permit the detector to see all areas in the target plane. The detector is mercury-doped germanium with a normal operating temperature of 30°K. Cooling is provided by a Malaker Mark 7 closed-cycle cryogenic cooler. The closed-cycle system offered significant advantages over the manually-filled helium system which was the alternate system.

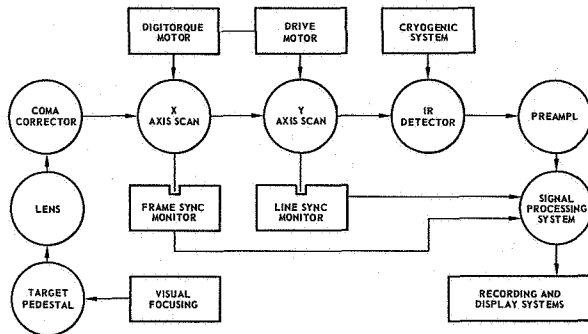


FIGURE 3. BLOCK DIAGRAM OF FAST SCAN INFRARED MICROSCOPE

A diameter of 20.3 centimeters (8 inches) was chosen for the primary lens, and the focal ratio was set at F 1.1. This long focal length enables the object to be away from the primary optics in a space of its own. It further permits the use of an off-axis system; the only aberrations from this system occur because the field is spherical rather than flat. However, under the conditions in which this device will be used, these aberrations are not a major factor. Optical resolution of a diffraction-limited characteristic is achieved in a lens system having a concentric, spherically round, germanium corrector and a spherical primary lens.

SCANNING SYSTEM

The high-speed, infrared microscope required a unique scanning system. This requirement was met by development of a polygon helix scanner in which a polygon, having 64 internal facets and 64 spaces, is rotated for the aperture mask of the detector at a speed of 1000 lines per second. This scanned beam is relayed to a pair of flat annuli oriented to fold the beam 180 degrees. Only a small segment of each annuli is used. The main effect is to provide the system with a corner reflector. This would be the effect if the annuli were perfect doughnut-shaped flat surfaces of glass; however, they are split with one end raised 0.381 centimeter (0.15 inch) to form a helix. When rotated together, these helixes transversely move the optical image as far as necessary to permit scanning a 1 1/2 millimeter surface at 10 Hz linear speed and 90 percent efficiency.

SIGNAL PROCESSING

Signal processing for the infrared microscope was made as simple as possible. The detector amplifier and log post-amplifier have variable gains and a variable bandwidth. To provide x and y drives for the cathode-ray oscilloscope or magnetic tape, synchronizing pulses come from both the polygon wheel and the helix wheels. The net result is an ability to provide a single frame image of the target to be scanned, as well as radiation amplitude versus time data on a continuous basis.

DISPLAY SYSTEM

The instrument's output is an analog signal having a maximum frequency of 100 Hz and the indexing of a video signal. Because of these characteristics, the output can best be connected to a conventional video tape recorder. Information from the video tape recorder can then be reproduced sequentially as video images on an oscilloscope, and line scans can be recorded directly on a strip chart recorder. In addition, information from the video recorder can be used as the input to an analog to digital converter, whose output proceeds into a buffer unit for storage and future computer processing.

The smallest elements of an integrated circuit are the junctions which can be only a few microns wide. Consequently, the area resolution of an adequate infrared system should be able to view them. Possibly an even finer resolution capability would be useful, but the wavelength of the radiation emitted by the target is the limiting factor. Therefore, the instrument was designed to have the following capabilities:

Area Resolution	20 microns
Temperature Resolution	1°K at 298°K ambient
Frame Composition	100 lines/frame
Scan Speed	1000 lines/second
Optical Magnification	7.6
Depth of Field	± 20 microns
System Efficiency	40%
IR Wavelength	6 - 12 microns

Once a microelectronic-device prototype has been built and is operating, a thermal map of it will enable the design engineer to verify that the thermo-electric stress is as calculated at every point of the unit. Electrical overstress, resulting in excessive power dissipation and thermal interaction thus causing unwanted heating of sensitive elements, will be apparent. Once these conditions have been pinpointed, design changes can be implemented and their effects verified on a modified prototype.

Thermal maps of production units can be compared with standards established for each basic device, and any significant variations during the production process will be apparent. From this information, suitable process changes can be made to correct the defects or anomalous devices can be discarded.

Figure 4 shows the circuit diagram and physical layout of a diode transistor logic dual 3 input gate that was evaluated for its thermal design characteristics. The location of every fifth line of scan of the fifty made is shown by the dotted lines. The size of this chip is 0.127 centimeter on each side (50 mil by 50 mil).

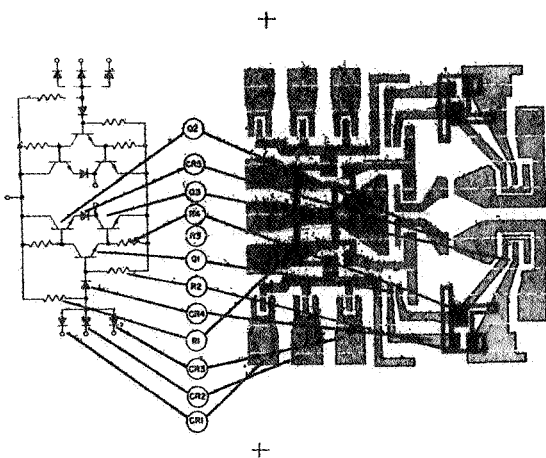


FIGURE 4. SCHEMATIC DIAGRAM AND PHYSICAL LAYOUT OF DUAL GATE

Figure 5 is a collection of the scope displays of each scan line of the fifty scans that were made.

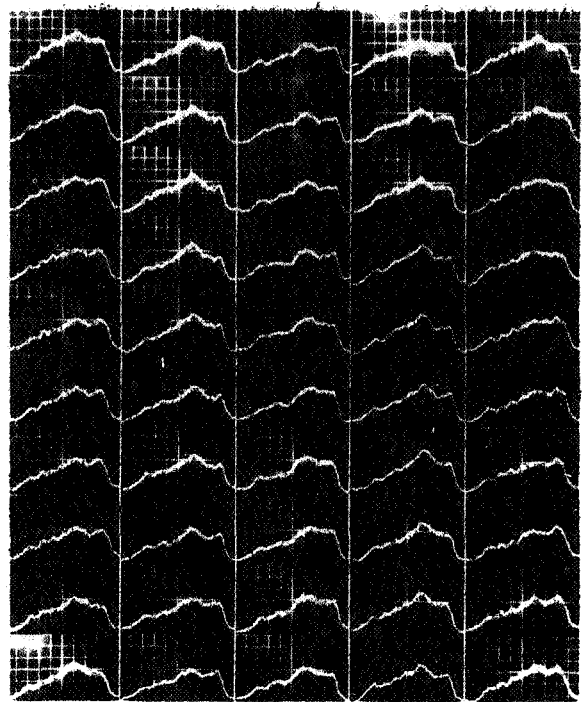


FIGURE 5. FIFTY INFRARED SCAN LINES OF MICROCIRCUIT

A cutout was made of each of the lines of scan and assembled into an IR profile of the circuit, as shown in Figure 6. By correlating Figures 4 and 6 you can relate the peak infrared emission to resistors and transistors within the chip. This analysis shows a maximum temperature rise in the circuit of 393°K with no major concentrations of heat. The evaluation indicates this circuit design has a relative uniform thermal gradient. Figure 7 shows a single line of scan superimposed over a layout of the circuit. The infrared radiation profile shows the location and temperature of the diode and transistor junctions and buried resistors in the chip.

Figure 8 shows a single line scan of a good circuit and a circuit with poor bond that was measured at 1, 6, 16, and 46 seconds during warmup. Warmup is rather slow in the good unit, so that at the end of 46 seconds the temperature has reached approximately 363°K. The temperature in the bad unit at the end of the same time has reached approximately 388°K. Under the infrared scan is an X-ray of the units that shows the void causing the elevated temperature. No voids are seen under the good circuit.

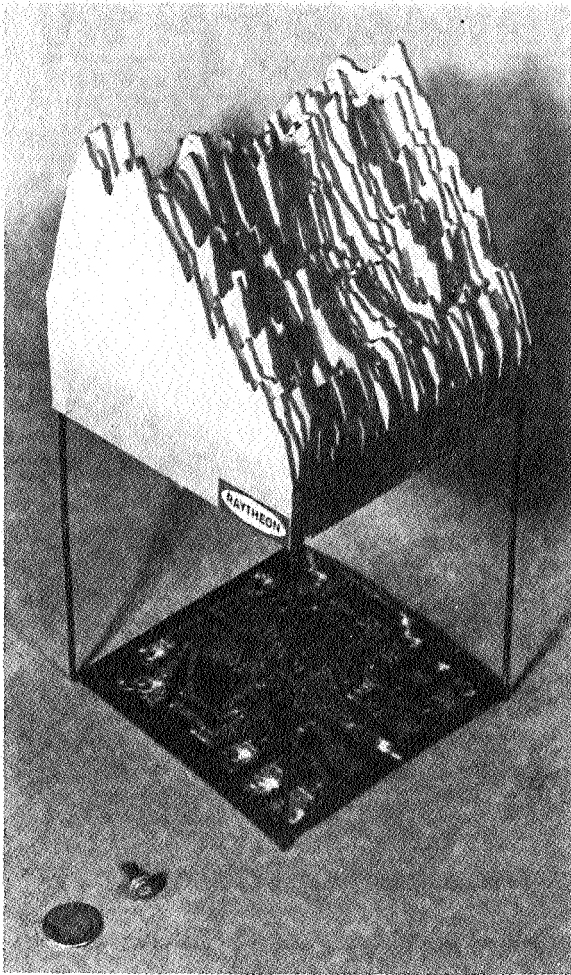


FIGURE 6. INFRARED PROFILE AND PHOTOGRAPH OF MICROCIRCUIT

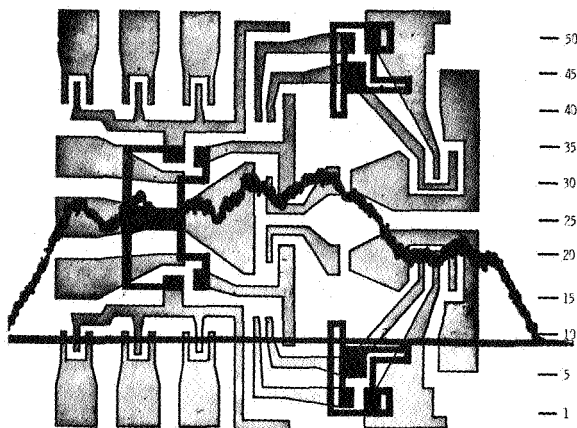


FIGURE 7. SINGLE SCAN IR SUPERIMPOSED ON CIRCUIT SCHEMATIC

Figure 9 depicts the scans made of a circuit containing a crack in the silicon. The scan line labeled initial warmup was made about 10 seconds after power was applied. This scan line shows a large drop in IR in the area of the crack.

The scan line made after thermal stabilization shows the same condition, but less pronounced. The defect is readily detected when initial power is applied, but not as easily detected after thermal equilibrium is reached. This is a good example of the need for an instrument to scan at a fast speed and have a fast response detector.

A study is in progress to determine the possibility of using infrared to predict transistors likely to fail because of second breakdown, and to pinpoint the area where the breakdown will occur. The 2N1722 power transistor used for this study is shown in Figure 10. The chip of this transistor is 0.635 centimeter (250 mils) square. The infrared profile of the transistor was measured just prior to driving it into breakdown and was found to be uniform and normal throughout the chip. The device was then driven into second breakdown and measured with the infrared microscope. The infrared spike shown in Figure 11 was found at the point of second breakdown. The breakdown occurred at a small point within the 0.127 centimeter (50 mils) square as shown in Figure 12, and there was deterioration around this point. This IR peak represents a spot temperature of more than 1073°K.

## FUTURE PLANS

The following investigations, using the infrared microscope, are being planned over the next 12 months.

1. Conduct detail studies of devices containing thermal related failure mechanisms to establish an explicit relationship between the infrared emission of these units and good units. From this information detailed test procedures and acceptance criteria can be developed for microcircuits.
2. Establish standards for the thermal and infrared design of microcircuits and detailed procedures for IR evaluation of circuits as a part of qualification and lot acceptance tests.
3. Locate the instrument in a microcircuit manufacturer's plant for approximately three months of testing to establish the relationship between effectiveness and efficiency of infrared testing of microcircuits in accomplishing the above functions.

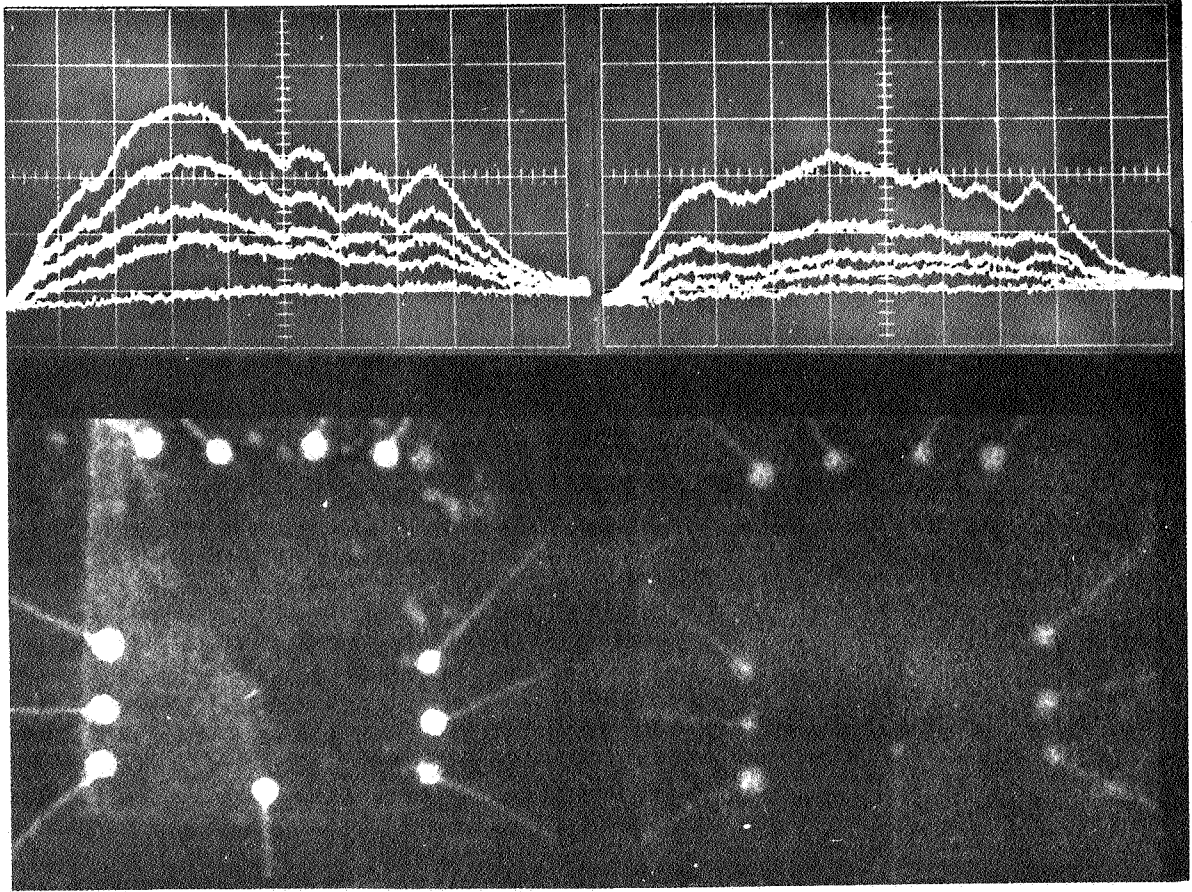


FIGURE 8. IR SCAN OF CIRCUIT AT 0, 1, 6, 16, 46 SECONDS DURING WARMUP AS RELATED TO X-RAY OF UNIT

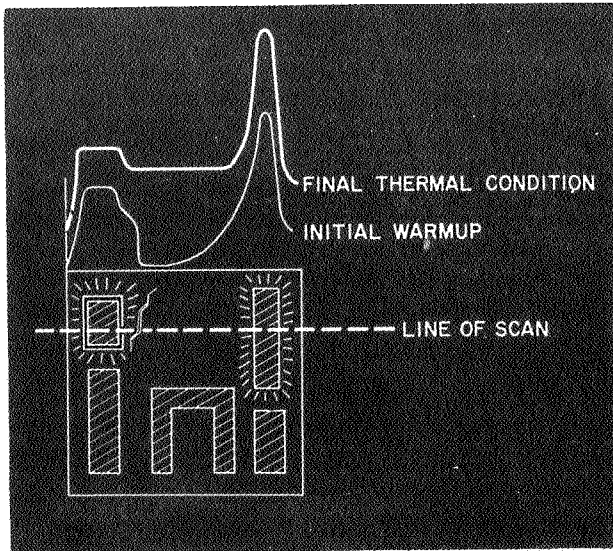


FIGURE 9. IR SCAN OF CIRCUIT WITH A CRACK IN THE SILICON

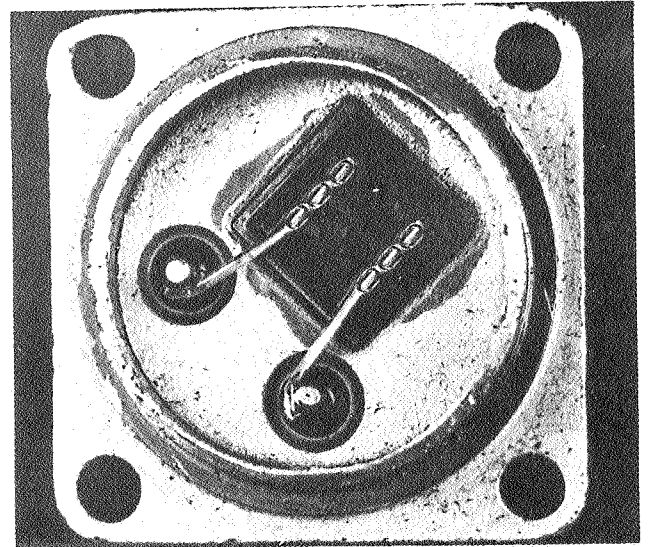


FIGURE 10. POWER TRANSISTOR USED FOR SECOND BREAKDOWN STUDY

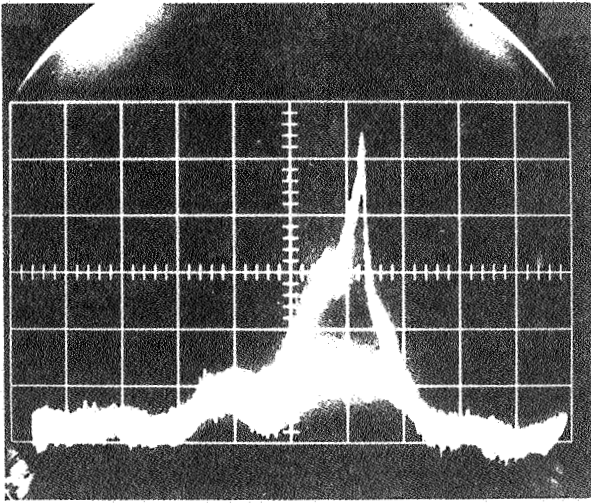


FIGURE 11. NORMAL AND SECOND BREAKDOWN INFRARED EMISSION

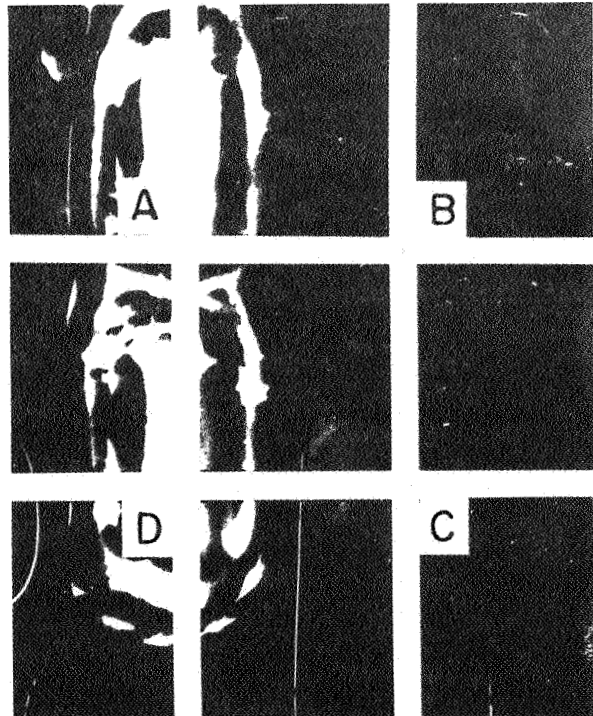
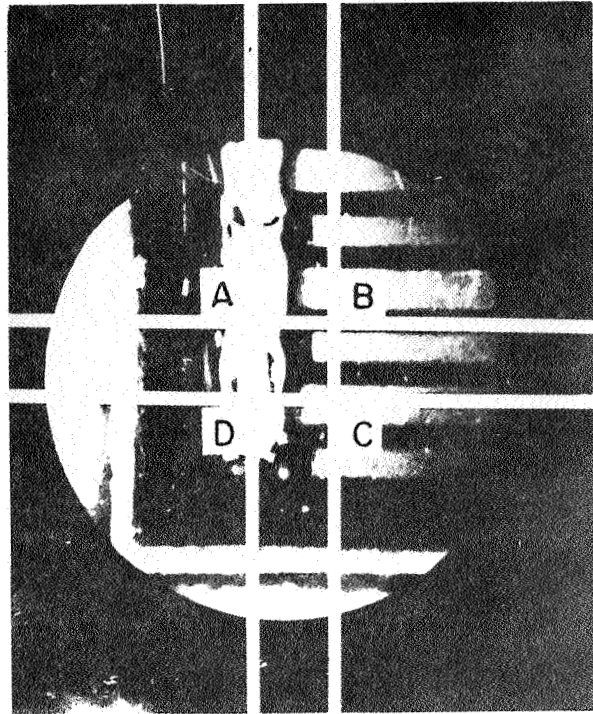


FIGURE 12. AREA WHERE SECOND BREAKDOWN OCCURRED



# USE OF SLURRIES FOR HYDROSTATIC TESTING

By

Frederic E. Wells

## SUMMARY

The hydrostatic proof testing of tanks to their full flight loads by the use of slurries is discussed. Guidelines for necessary slurry characteristics are established. Slurries to meet these NASA criteria were developed and evaluated by the Georgia Institute of Technology. Tests were conducted for slurry viscosity under shear stresses, for exposure to sunlight, for compatibility with two cryogenic liquids, and for corrosion on various tank surface materials. The economics of producing slurries with the required specific gravity is mentioned. The usefulness of further experimentation by using a pilot plant is explained.

## INTRODUCTION

Proof testing of propellant tanks to full load is necessary because of the very narrow margins imposed on vehicle designs by weight considerations. These designs have resulted in tanks with yield to design load ratios of 1.1 to 1.0. Any defects in raw material or fabrication can result in a disastrous failure during static firing or in flight. In-process inspection will detect most defects; however, only a full load proof test can give the assurance required for a major vehicle, especially if it is manned.

Heavy propellant in a boost situation causes a much steeper pressure gradient than that of a proof test using water in a 1 g static environment. As an example, lox in a 4 g boost causes a gradient of  $4.18 \text{ N/cm}^2$  per meter of tank height (1.99 psi per foot of tank height). This is four and a half times the gradient that can be produced with water in a static proof test. This means that a lox tank 19.7 meters (60 feet) in length would have a pressure gradient between forward and aft bulkheads of  $82 \text{ N/cm}^2$  (119 psi) in a 4 g boost, while the pressure gradient that could be produced by a water static proof test would only be  $17.9 \text{ N/cm}^2$  (26 psi).

It is apparent that a lox or RP-1 tank cannot be tested to actual flight loads with water without

causing a serious overload on the upper bulkhead and upper portions of the tank. The result is an untested tank or a tank overdesigned (with a resulting weight penalty) to meet the requirements of hydrostatic proof testing. This is not a problem on the older designs with constant wall thickness; however, increased tank size has made the tapered wall thickness designs look very attractive for weight reduction.

The desirability of carrying the tapered wall design to the ultimate, combined with the necessity of a 100-percent proof test, has led to considerable work to develop methods of achieving pressure gradients to match anticipated flight loads. One solution was the zone gradient method that was developed at MSFC and reported in document IN-R-QUAL-64-43. This method is feasible within the following limitations: (1) it cannot be used on a tank other than a basic cylinder, and (2) a given set of fixtures can only be used on one diameter tank. A change in tank diameter requires a complete new set of fixtures.

A concept that would not require fixtures for the tank and would be adaptable to any tank configuration was still needed. An obvious solution would be the use of a fluid for the test media that would be dense enough to produce a pressure gradient matching the flight loads. A true liquid that possesses the characteristics for this type of proof testing does not exist; however, the concept of slurries was believed to be worth investigating in detail, and a contract was awarded to Georgia Institute of Technology to investigate this approach.

## CRITERIA FOR SLURRIES

To meet the requirements for proof testing, a slurry must be capable of being produced with a specific gravity range from 2.0 to 6.0; be chemically stable; be nonsettling for extended periods of time; be inert to liquid oxygen, liquid nitrogen and hydrocarbon fuels; transmit hydraulic pressure as does a true incompressible fluid; be compatible with stage component materials; be readily prepared and pumped with conventional processing equipment; and be easily removed from tanks and piping by water flushing.

To be economically feasible, finished slurry formulations must be reasonably priced and composed of such readily available materials that purchases of large quantities would not seriously disturb existing markets.

## GEORGIA INSTITUTE OF TECHNOLOGY STUDY

This study was to develop high density slurries with specific gravities from 2.0 to about 6.0 to be used as the pressure transmitting media in the hydrostatic testing of stage propellant tanks. Slurries meeting specific gravity requirements were to be thoroughly tested and characterized, and recommendations were to be made for suitable types of equipment for the preparation, pumping, and storage of the slurries.

An extensive survey of the chemical and physical properties of a large number of dense, granular solids revealed several solids that possessed many of the properties desired for the purpose of this study. Water was selected for use as the continuous medium in the slurry formulations, principally because it is relatively inert, cheap, and plentiful.

Water-based slurries were formulated from a large number of materials, and it was conclusively shown that specific gravities from 2.0 to 6.0 could be achieved with conventional chemical processing equipment. Lead oxide was the most suitable of the solids tested for producing stable slurries with a wide range of specific gravities. Barium sulfate slurries also demonstrated very favorable characteristics for the lower densities. The necessary particle size distribution, the optimum type and amount of dispersing agent, and a suitable preparation procedure were developed for producing these slurries.

Different types and amounts of dispersing agents were used to determine the optimum. The type and amount of primary dispersing agent used determines the polarity of the slurry and, to some extent, the viscosity.

Several thickening and gelling agents were also evaluated. The goal was to select an agent that would completely disperse the solid particles and then select a second material to establish a weak gel structure in the slurry. A weak gel structure established under static conditions will greatly impede solids settling and result in a soft, readily redispersible sludge when significant settling has occurred

after long-term storage. A slurry thus formulated will be rather viscous yet flow readily when shear is applied.

Since slurries are inherently non-Newtonian in character, apparent viscosities at various shear rates are often necessary to specify their flow properties. Measurements of this type are also frequently needed to define time-dependent flow properties such as thixotropic or rheopectic behavior wherein shear-stress varies with time when a constant shear rate is applied to the slurry. Controlled thixotropy is a very desirable characteristic for maintaining stability against particle settling under static conditions and yet permitting reasonable viscosities when a shear gradient is applied to the slurry. These are reversible phenomena; that is, it reverts to its original gel-like structure when shear stresses are removed.

Since apparent viscosity is a primary factor determining stirring and pumping costs and apparent viscosity varies with the rate of shear, the apparent viscosity of each slurry was determined at the same rate of shear to give a basis for comparison in determining the optimum amounts of the dispersing and gelling agent.

Several different types of agitation systems were evaluated. These included propellers, paddles, turbine impellers, and high-shear twin blade homogenizers. A turbine-type impeller located very near the bottom of the mixing container gave the best combination of fluid shear and circulation needed for dispersing large quantities of solids. The use of hot water improved the rate of solids wetting and also resulted in lower power requirements for mixing because of decreased slurry viscosities at elevated temperatures.

## PERFORMANCE TESTS ON LEAD OXIDE AND BARIUM SULFATE SLURRIES

Direct exposure of lead oxide slurries to sunlight caused a series of color changes from bright yellow to a dull red-brown. In some instances, the color further changed to black upon prolonged exposure to sunlight. These color changes occurred only within a very thin layer at the surfaces of the sample containers. These darker films were somewhat more difficult to remove by water rinsing than the usual film, but otherwise presented no difficulties. No measurable density alterations were noticed after these changes occurred. Examination of a Pourbaix diagram for lead and water reveals that litharge is

the most stable state for lead at these pH levels, so very little overall change in oxidation states would be predicted.

Tests conducted with liquid nitrogen and liquid oxygen indicate that deposited slurry films are completely compatible with these liquids.

Hydrostatic pressure testing at local barometric pressure and at elevated pressures demonstrated that the slurries possessed the required fluid characteristics to transmit hydraulic pressure.

Wet slurry films were easily removed from aluminum and glass surfaces by rinsing with cold water. However, if the lead oxide films were allowed to dry, removal was considerably more difficult and some abrasive action was often required.

In the corrosion tests, stainless steel and aluminum alloy samples were partially and totally immersed in the slurries for extended time periods, i. e., 12 to 21 days. The stainless steel samples showed no reaction to this immersion. The untreated aluminum sampled did show some reaction after extended immersion. This reaction consisted essentially of a reduction of the lead oxide in contact with the aluminum surface to yield a surface film of lead and lead oxides. The most obvious way to minimize this type of reaction is to adjust the slurry pH to neutral. Anodized aluminum samples showed no significant reaction.

## ECONOMIC CONSIDERATIONS

A preliminary economic analysis indicated that barium sulfate slurries are desirable for specific

gravities to about 3.0. Lead oxide slurries are recommended for specific gravities above 3.0. The economics of purchasing the required quantities of the slurries from commercial suppliers were compared with those of building an onsite processing plant for producing the slurries. This preliminary analysis favors the construction of an onsite facility.

## FUTURE PLANS

The Georgia Institute of Technology has clearly demonstrated the feasibility of producing slurries that can be used for hydrostatic proof testing of flight tankage to full flight loads. Small-scale model testing of these slurries is needed. These tests would be conducted under conditions dynamically similar to actual operating conditions. The high density slurries developed in this study should also be examined periodically for possible destabilization or stratification with formation of a density gradient. The unfavorable tendency of high pH slurry solids to decompose when in contact with aluminum alloys remains a possible disadvantage to their use as proof testing media. Additional corrosion studies are needed to solve the above problems and to determine the construction materials to use in slurry production facilities. Pilot plant studies should also be performed to determine the type of materials, equipment, and processing procedures that would be most feasible for producing large quantities of slurry in an onsite facility.



# AUTOMATED ULTRASONIC SCANNING BY TRIANGULATION METHODS - THE DICKINSON SYSTEM

By

Robert L. Brown

## SUMMARY

The advantages of ultrasonic testing compared with previous nondestructive test methods are discussed. The capabilities of an "acoustic spectrometer" are demonstrated in a practical test on a section of S-IC fuel tank. Operation of the acoustic spectrometer by servos rotating the transducers that supply the computer with position information is explained. The location of the transducers and the computer's method of locating flaws in welds through scattered ultrasonic energy is discussed. An accurate method for examining welds and verifying the existence of detected flaws is presented\*. The system's accuracy and automated operation by remote control are mentioned as ideal qualities for repetitive examination of a ship's hull or a nuclear reactor where severe service conditions exist.

## INTRODUCTION

Perhaps the oldest nondestructive test, other than visual examination, is sonic testing. It still remains a valuable and valid test for quality in non-critical applications. The test lacks sensitivity because of a fundamental reason. If a flaw is to be detected by its influence on frequency and resonance, it must be large in relationship to a wavelength of the frequency generated. Middle "C," which is in the mid-range of frequencies where our ears are most sensitive, has a wavelength greater than 2.3 meters (7 feet) in the common engineering metals. Since rejection limits for flaws in critical applications are normally specified in microns (thousandths of an inch) in cross section, detection by sonic testing using audible frequencies is not possible.

The solution to detecting flaws can be provided by ultrasonic testing. Equipment capable of generating and detecting sonic frequencies in megahertz (millions of cycles per second) is standard, and within these frequencies, wavelengths in microns

(thousandths of an inch) allow any reasonable limitation on flaw size to be met. It is common practice to operate ultrasonic testers at a level of sensitivity that allows flaws smaller than the rejectable size to be identified. This capability has made ultrasonic testing a recognized nondestructive testing method.

The major handicap in ultrasonic testing is scanning speed. The pulse rate must be slow enough to be clearly differentiated by electronic means from shot-type noise, and travel speed must be slow enough to allow interrogation of each flaw by at least three pulses. To be consistently free of phantom indications requires an almost ideal system.

The high degree of acceptance of conventional ultrasonic testing methods may lead to a tendency to disregard unconventional testing possibilities. Recently, a West Coast company was developing an ultrasonic testing system unique in many important concepts. These concepts, while new to ultrasonic inspection devices, were well established in other applications and would hasten the inspection of many of the welds in the Saturn V system. This potential led the laboratory to contract for a system specifically engineered for space vehicle applications. This system, the acoustic spectrometer, is now being evaluated inhouse to further determine the capabilities and limitations of the system.

## ACOUSTIC SPECTROMETER

Figure 1 shows the acoustic spectrometer set up in the evaluation laboratory. A panel that has a configuration duplicating a section of the 10.8-meter (33-foot) diameter S-IC fuel tank is shown. The required tooling is being attached to the test panel. This tooling was designed for use in the production application referred to earlier. A horizontal weld may be seen extending across the top third of the test panel and a vertical weld at the center. These welds contain flaws which have been precisely

---

\* Evaluation of this equipment is continuing.

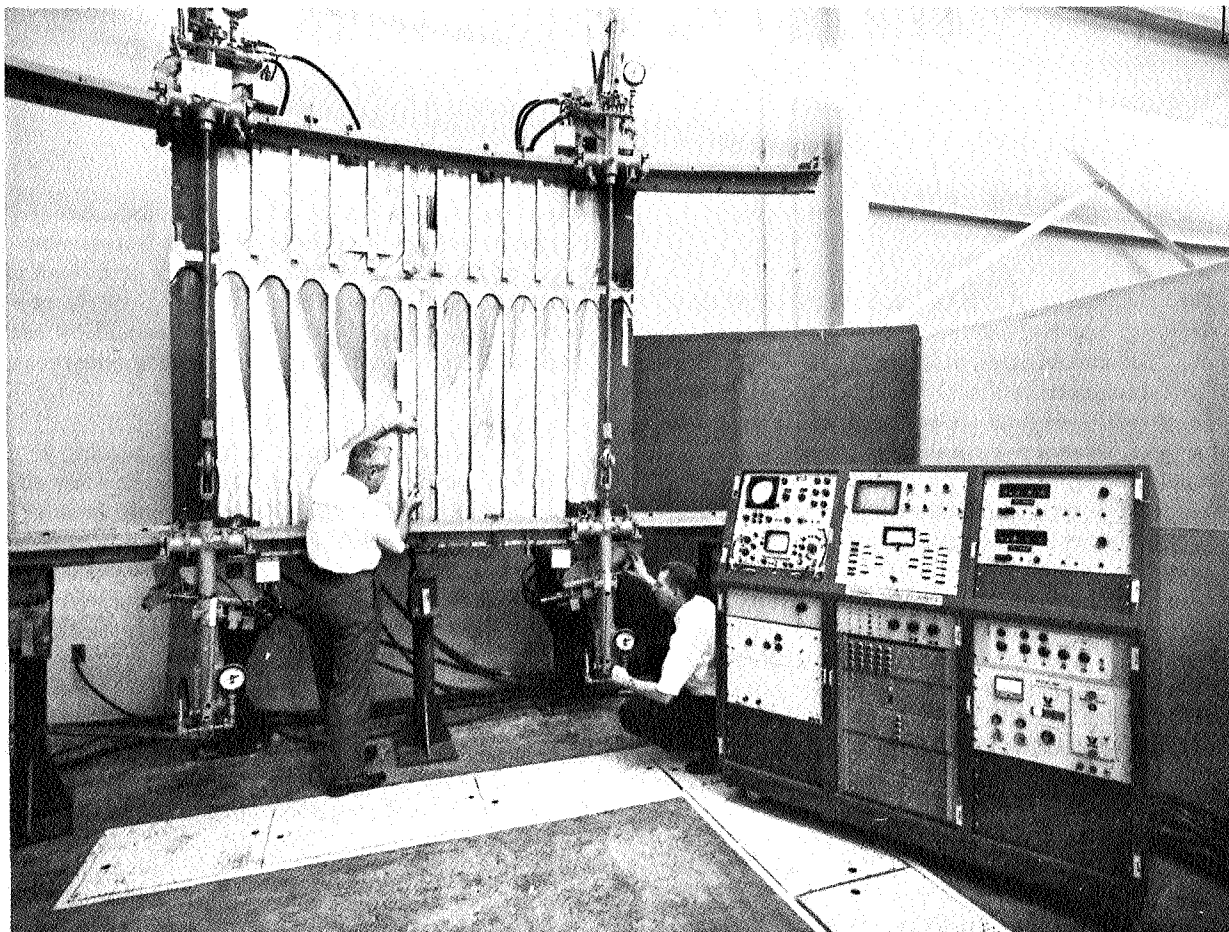


FIGURE 1. ACOUSTIC SPECTROMETER INSPECTION OF S-IC FUEL TANK SECTION

located and evaluated by X-ray and conventional ultrasonic methods. This simulates a test that would normally be performed on the cylindrical tank section. Prior to welding to the bulkhead assemblies, all welds in the vertical and circumferential directions would be inspected, repaired if necessary, and accepted, without moving the ultrasonic transducers from their locations.

The acoustic spectrometer differs from the conventional ultrasonic tester in that it is much more complex, as a necessary consequence of the new approach taken with respect to data acquisition and analysis. This increased complexity is reflected in the console shown to the right in Figure 1. The acoustic spectrometer is classified as a pulse system in which one transducer acts as a transmitter, and one or more receive information in the form of ultrasonic energy scattered from flaws.

All transducers (this system has provision for five) are identical and can be programmed to act

interchangeably as transmitters or as receivers. The system does not use the "single crystal" mode of operation in which one transducer acts as both transmitter and receiver.

Instead of shock excitation by single pulses, the transducers are driven by widely spaced pulse bursts which are variable in amplitude, duration, and spacing. The burst frequency is independent of pulse spacing. The duty cycle is low, always under one percent, which permits 1500 volt excitation without harm to the titanate transducers. The resultant, highly damped wave train of ultrasonics is at the frequency of the burst and can be tuned over a wide range. This ultrasonic energy is fed into a system of acoustical lenses and directors where it is narrowed into a highly collimated beam inside an acoustic waveguide. This unit is coupled to a wave director so that it may be rotated around a quadrant of a circle by a hydraulic servo. The unit will transmit a very narrow beam of sound into an attached plate, acting as a rotational, highly directional

acoustic antenna, which has the same directional pattern in receive or transmit modes. As an aid to visualization, use of the terms "transmitted" and "received" beams is a convenience found helpful in working with this equipment.

Figure 2 is a sketch of a typical setup using four transducers. The sonic ray traces are sketched in

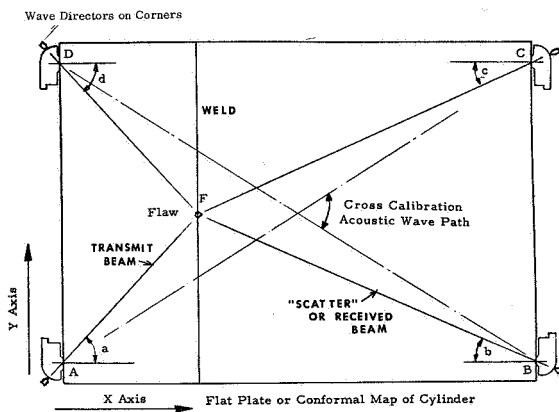


FIGURE 2. LOCATION OF FLAWS BY MULTIPLE WAVE DIRECTORS

to illustrate the triangular pattern of distances and angles that the computer solves in locating flaws. Positioning of the transducers is important because the basis of the computer's calculations for location of flaws is the accuracy of the base distances from which the locations of the intersections of the transmitted beam and the received beams are computed.

Oscilloscopic studies indicate that the shell is shock excited into compression waves, resonant in the thickness mode - symmetrical Lamb waves - and the conversion is highly efficient if the input ultrasonic excitation frequency approximates the resonant frequency of the plate thickness. The particular shell panel which is presently set up in the acoustic spectrometer was found to respond to the following: burst frequency, 2.32 megahertz; burst width, 150 microseconds; 150 bursts per second, and 1,000 volt peak excitation to the transducers.

The wave directors are coupled into the shell by soft metal shims under high compression which so effectively bridge the gap between plate edge and wave guide that the acoustic impedance is negligible. This coupling transfers perhaps 10 times the sonic

energy as a fluid. Tests have shown no benefit from fluid in this joint. The clamping force is obtained from hydraulic actuators which are preset to exert the correct pressure.

Figure 3 is a block diagram of the acoustic spectrometer system. A transducer and its functional parts are shown to the right of the blocks which indicate the control and display functions. The computer is the heart of the system. This is a small analogue three-channel computer, each channel identical in its circuitry. The transducer-to-transducer distances are manually set into the computer's input in the form of voltages taken from precision potentiometers. The transducer angle positions that are required to calculate the X and Y coordinates of the intersect point of the transmit and receive beam are controlled by voltage feedback from tangent potentiometers attached to the pivots of the wave directors.

The computer continuously solves the equations of position for all transducers and feeds this angular information into the servos on each transducer separately. Each servo rotates its transducer to an angle that gives an output voltage on the waveguide tangent potentiometer that, fed into the computer, satisfies the equation of position that the computer is continuously solving. Since all active transducers are positioned by their independent computers, all transmitted and received beams remain pointed at the calculated intersect point. The computer's calculated coordinates of this point are read out as X and Y distances by a pair of digital voltmeters in inches and decimals of an inch. This intersect point is where the "scatter" that carries useful information originates. A toggle switch, which has four independently closed positions, switches driving voltages to the appropriate circuit to move the intersect in the direction indicated by the position of the handle; plus or minus X, or plus or minus Y. The motion is constrained by the computer to move in X or Y directions only. No combination of these motions is possible, but combinations of sequences of X and Y motion allow all areas to be covered to any degree of thoroughness required. This constraint is a great advantage when welds, such as the S-IC circumferential welds, lie completely in the X or Y direction. The beam is steered by sequential moves in the X and Y direction to the correct starting point as shown by the coordinates displayed by the digital position indicators. The computer will then steer the intersect along the weld until the limit of the scan is reached. This directing system is quite accurate; the preliminary data indicate that an error in angle is less than one degree.

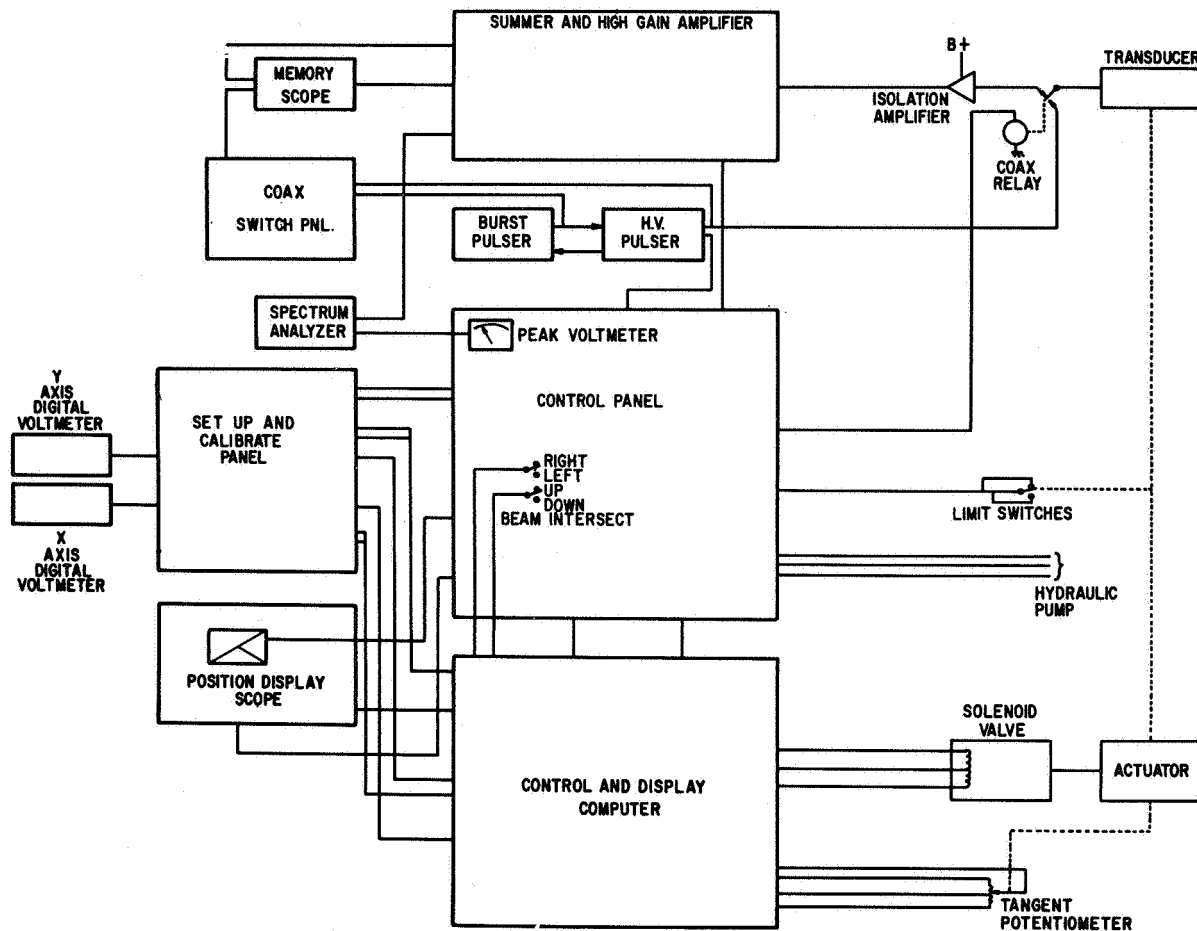


FIGURE 3. BLOCK DIAGRAM OF ACOUSTIC SPECTROMETER SYSTEM

A second position indicator in the form of a cathode ray oscilloscope is provided at the top of the center panel. This oscilloscope displays the ray paths followed by the ultrasonic beams in the structure as generated by those transducers active at the time of display, allowing visualization of directions, travel, and position, all of which are difficult to handle without such an aid. A coordinate grid on this readout giving distances in feet was used during the evaluation. Since the display was for all practical purposes a "real time" readout, this display was the preferred means of monitoring the ultrasonic system while the operator is "steering" by the four-way switch.

While "intersect point" is mentioned frequently, the word "point" is a convenience and is not intended to imply that a point can be resolved. A flaw such as a small round pore can be located within a small circular area which is the "limit of resolution" for the system. This circle may be approximately 2.5-centimeters (1-inch) in diameter at 3.3-meters

(10-feet) distance from the transducers. When the acoustic spectrometer is used to evaluate welds, which may contain only an occasional rejectable flaw, this circle is a small enough limit. To verify the exact location of the flaw, a conventional portable ultrasonic tester will pinpoint the exact position.

An important feature of the system is a time-dependent gate that can be set to receive "scatter" from the intersect point, and which can block "scatter" from other parts of the plate. This suppresses the background noise in the system, thus increasing the strength of the flaw signal.

Flaw analysis is an integral part of flaw detection. The acoustic spectrometer is equipped with several devices which aid in this important function. Since the system is intended for highly automated operation, primary reliance in flaw detection is on a spectrum analyzer which reduces the flaw return information to a voltage that is fed into a peak-reading voltmeter. The peak voltage from the flaw

signal return is then compared to a preset reject level set at the smallest rejectable flaw size. The system will give an indication at each detected flaw having a cross section larger than the preset limit. The operator analyzes each flaw by confirming the automatic flaw signal indication on a cathode ray oscilloscope. This oscilloscope presents the conventional time base versus amplitude, with the exception that the time gate only allows the "first reflection" or "scatter" signal to be displayed. The time gate is opened enough to allow the conditions along the weld to be shown on the oscilloscope, and analysis is a function of the operator's skill and experience in interpreting the changes in the pattern as the intersect point travels through flaws. This

analysis is then applied to evaluate the reject circuitry and to evaluate the system as a whole.

Equipment closely related to the acoustic spectrometer can perform such tasks as routine ultrasonic examination of plates in the rolling mill. With tape input and recorder outputs, ultrasonic devices could be used to search for hull damage on ships and to monitor reactors where severe or dangerous operating conditions exist. A highly automated ultrasonic system could perform a nondestructive testing task on a routine, repetitive basis in situations where conventional ultrasonic testers cannot be used.



# ULTRASONIC EMISSION DETECTOR EVALUATION OF THE STRENGTH OF BONDED MATERIALS

By

James B. Beal

## SUMMARY

A program to measure adhesive bond strength was conducted. A study into the causes for weak adhesive bonds was made to determine the best methods of nondestructive testing of the adhesives. The discontinuities in the bond layer are discussed and related to ultrasonic signals. Bond stress methods and possible test techniques are listed. The measurement of bond strength by producing consistent weak bonds and the causes for the weak bonds are discussed. Fabrication of test samples are presented.\* The operation and capabilities of the ultrasonic emission detection equipment are explained, and the advantages and disadvantages of the equipment are listed.

## INTRODUCTION

Aerospace industry requirements have rapidly accelerated the use of adhesive bonding in structural applications. Composite structures, particularly those using honeycomb, are to a large extent adhesive bonded today. The major problem posed by the use of composite structures has been the variability of bond strength obtained and the lack of suitable nondestructive equipment for determination of bond strength. The exact causes of these strength variations are difficult to establish because the causes can be related to every phase of bonding, i. e., material properties, material and adhesive handling, and processing techniques (Table I). The soundness of an adhesive bonded assembly must be assured by two methods. One is the verification of every phase of bonding, commonly called process control, and the other is end-item evaluation (final inspection).

\* The Ultrasonic Emission Detector and the methods of equating the noise signal level of a stressed bonded structure to an indication of bond strength were developed by testing these samples.

Contract NAS8-11456, "Nondestructive Testing For Evaluation of Strength of Bonded Material," was initiated June 29, 1964, with General American Transportation Corporation [1]. This contract was to develop a nondestructive method or system for evaluating adhesion bond strengths in composite adhesive bonded structures. Acceptable methods for detecting bondline voids, debonding, bondline variations, and porosity were available at that time, but no nondestructive techniques were available that would measure adhesion bond strengths in all adhesives specified for this program, i. e., FM-1000, HT-424, Narmco 7343/7139 and Metlbond 329. These adhesives were used to make specimens of aluminum bonded to aluminum; aluminum face sheets to aluminum honeycomb core, and aluminum face-sheets to phenolic core.

TABLE I. REDUCTION OF BONDING PROBLEMS  
BY USING NONDESTRUCTIVE TESTING

Causes of Bonding Problem	% Without NDT	% Using NDT
1. Design Deficiencies	30	25
2. Corrosion	7	5
3. Machining Errors	10	0
4. Improper Processing	9	0
5. Misuse or Handling	10	5
6. Fabrication Error	12	0
7. Material Defects	22	0
	<u>100%</u>	<u>35%</u>

The literature survey phase of nondestructive testing revealed that the number of papers published on the subject of bond strength evaluation, for the adhesion strength of the bondline, were relatively few. Available papers were concerned with particular equipment for detection of voids, delaminations, porosity, bondline variations, and the cohesive strength of some adhesive systems, but the equipment was inadequate for detecting weak bonds in adhesion. The need existed for a bond strength

evaluation system and a method of producing consistently poor adhesion bonds of predictable values in order to adequately evaluate equipment bond strength indications.

## ADHESIVE BONDING

Adhesive manufacturers and users agree that strict controls are necessary over all adhesive bonding processes and the numerous associated fabrication variables. Considerations for a good bond include the formation of a strong wettable oxide surface on the metal to be bonded, proper wetting of the surface with the adhesive, elimination of contaminants, and control of the fitting, temperature, and pressure of the bond.

The majority of present nondestructive test instruments fall within two categories: (1) vibration inputs to structures by means of resonant, sonic, and ultrasonic frequencies, and (2) structural proof stress tests consisting of internal pressurization, external tension stress induction, and limited destructive shear. A study was conducted into the nature of bonding to determine what properties affect adhesive bond strength and to determine the nondestructive test technique best suited for the measurement of strength properties. The apparent failure of an adhesive bond was attributed to causes such as surface contaminants of a low cohesive force, or of chemical compositions that weaken the layer of adhesive near the surface. The cause of weak bonds did not appear to be the weakening of the basic bond forces, but rather the failure to form the bond in the first place. Thus, the strength of the surface layer of the adhesive was more important than the nature of its bonding forces. Any contamination affecting the strength of the first layer of adhesive was very important. Small areas of contamination can cause stress risers that propagate cracks parallel with and close to the bondline.

If the contamination and discontinuities in the bond layer cause stress risers and contribute to the failure of a bond, it is possible to have complete adhesion over the greater portion of an area and still have a weak bond not detectable by other nondestructive means. It was assumed that detectable sonic and ultrasonic signals would result from stress concentrations in contaminated areas of the samples before the stressed bondline reached the point of failure. Noise emission from stressed areas would result as the weak bonds failed selectively in the areas of highest stress.

## EVALUATION OF ADHESIVE BOND STRENGTH

The possibility of small contaminated areas being able to affect the total bond strength indicated that some method of stressing the bondline to fail the weak areas would be necessary. Because the small contaminated areas will be exposed to very high stresses when the bondline is loaded, the areas will emit sonic and ultrasonic signals that can be detected by sensitive listening devices long before the complete bondline reaches its ultimate strength. This phenomenon will provide additional data during proof tests of edge-sealed sandwich structures containing perforated honeycomb core, and during static load tests of adhesive bonded brackets.

Theoretical and bond stress methods considered for this program were: (1) rapid decompression of samples containing perforated honeycomb core, (2) high pressure external to a vacuum cup on a bonded structure containing a perforated honeycomb core placed in a pressure chamber, (3) electrical bond stress methods from forces produced by stationary charges, magnetic fields, and eddy currents, (4) force pulses by vibration and energy transfer to the bondline (forces produced by ultrasonics and shock wave stressing), and (5) mechanical methods by static or dynamic loading of bonded brackets or the structure.

Test techniques to be investigated for this program were: (1) sonic and ultrasonic emission detection of signals from failing bonds, (2) ultrasonic attenuation with applied stress, (3) brittle coatings, stresscoat or equivalents, and (4) birefringent photoelastic plastic coatings.

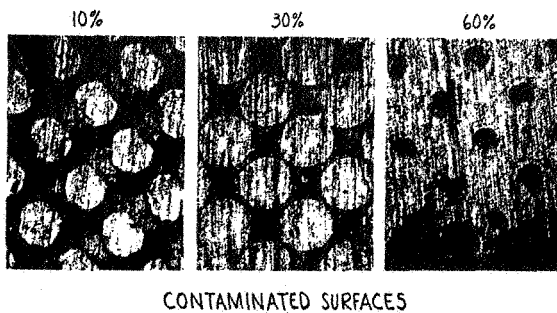
In any nondestructive test system, an important consideration is the production of sample flaws. This is particularly difficult in the testing of bond strength because the flaw mechanism relationships are not clearly known. In practice, poor bonds can be caused by a failure in the cohesive strength of the bulk of the adhesive or in an adhesion failure to the faying surface. These failures occur because of material and structural variations. If the structural materials and adhesives have suitable material properties, the unsatisfactory bonds which cause failures and which must be detected by the inspection system seem to result from: (1) improper cleaning and etching as a result of contaminated cleaning and etching baths or inadequate process controls, (2) a weak interface in the bondline may be present from contamination such as moisture or surface oxides caused by long-time surface exposures before

priming or applying the adhesive, (3) degradation of the adhesive material's cohesive strength. This may occur adjacent to the bondline because of contamination of the adhesive with moisture or other chemicals, or poor cure and fit-up practices, and (4) small contaminations that act as stress risers can cause the failure to progress along the bondline. The various contaminants are introduced at every stage of fabrication until the structure is complete.

The above conditions must be simulated as closely as possible to produce suitable imperfections affecting bond strength. Attempts to simulate under-strength bonds produced a successful method, designated photomicroflaw, which was used for controlling bondline strength of test specimens.

Other methods of bond contamination that were investigated and found unsuitable because of lack of predictability were: (1) exposure of face sheets to water solutions, (2) exposure of face sheets to oils and greases, (3) variation of face sheet cleaning methods, (4) exposure of cleaned, protected face sheets to long time storage conditions, and (5) partial cure or aging of the adhesives.

The photomicroflaw technique involves coating the surfaces of specimens to be bonded with a photo-sensitive emulsion and exposing the surface to an intense light source through a grid (Fig. 1). The



CONTAMINATED SURFACES

FIGURE 1. PHOTOMICROFLAW TECHNIQUES

emulsion is washed away by the developer at the areas where light is stopped by the grid. Photographer's screen-tints, the size and density controlled dots on a polyester film base, are used for the grid. This satisfies the need for simulating poor bond strengths through controlled surface contamination.

The importance of proper process control during bonding operations is shown in Figure 2. This

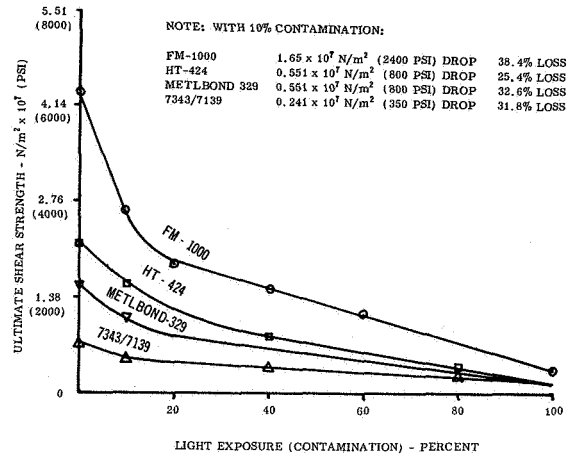


FIGURE 2. PHOTOMICROFLAW CONTROL OF BOND STRENGTH WITH LAP SHEAR SAMPLES

graphically illustrates the effects of bondline contamination on bond strength. Adhesive bond strength drops of twenty-five to thirty-eight percent occur when a surface to be bonded is degraded uniformly by ten percent contamination. This indicates that the higher the bondline stress, the more effect a small defect, debond, or weak bond can have as a stress riser. This significantly illustrates the need for contamination control in the process of fabrication. Assembly of components should be performed as soon as possible after the cleaning operation has been completed.

During this program it was noted that thirty to forty percent bond strength reduction occurred for cleaned face sheets which were protected against surface contamination and stored for one month prior to test sample preparation with FM-1000 adhesive. These results also gave emphasis to the rigid holding time and handling requirements for cleaned parts prior to adhesive application, assembly, and cure.

Specimens with bonds of known strength are required for suitable evaluation of nondestructive test equipment developed for this program. The development of confidence in production of specimens with controlled bond strengths requires destructive tests in accordance with established specifications. All specimens for this program, lap shear, drum peel, flatwise ring tension for metal-to-metal tests,

and other specimens required, were prepared in accordance with military specifications for bonded structures [2,3]. In the flatwise ring tension tests (Fig. 3), specimens were made from three inch

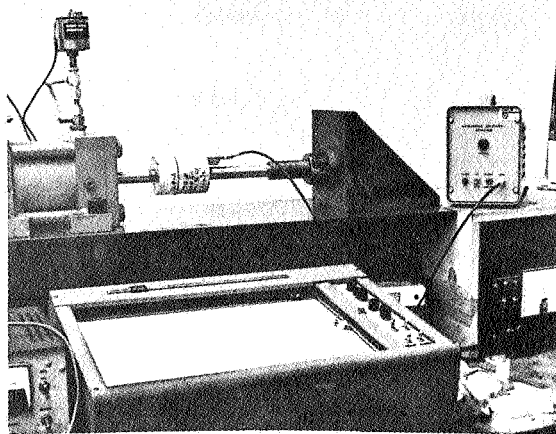


FIGURE 3. FLATWISE RING TENSION TEST APPARATUS

diameter cylindrical aluminum blocks. Two blocks were required for each test specimen with one block containing a central machined recess. These specimens were prepared in order to represent metal-to-metal bonded laminate construction and bonded brackets.

No problems were encountered in the preparation of test samples with the exception of the Narmco 7343/7139. This is a two component adhesive which requires mixing before use, and many problems were encountered in producing samples. The material is very sensitive to ambient environmental conditions. The variability of this adhesive is well known, however, it is the best cryogenic adhesive available. Because of the difficulty in preparing samples, this adhesive was not used in the equipment evaluation tests. The adhesive's room temperature elasticity precluded testing by the ultrasonic emission detector. It may be possible that further tests, conducted at the cryogenic operating temperatures normally associated with this adhesive, would produce useful data.

Adhesion bond strength degradation was attempted by environmental exposures of samples to high temperature of 533°K (500° F) for two hours, low

temperature of 84.2°K (-308° F) for two hours, and vacuum exposure to  $1.07 \times 10^{-4}$  N/m<sup>2</sup> ( $8.0 \times 10^{-7}$  torr). No degradation of bond strength was discernable by either nondestructive or destructive test.

To evaluate metal-to-metal adhesive bonds, test samples were fabricated using cylindrical aluminum blocks with annular recesses for ring tension flatwise tests. The transducer was attached to the cylindrical block by a threaded stud. The first few samples were broken so the operator, while listening with the headphones, could become familiar with the sounds preceding bond breakage. The bond force on the remaining samples was increased to the point just prior to bond breakage, as judged by the operator. A ten percent increase of this maximum force applied to the bond was considered the predicted bond failure point.

The application of ultrasonic emission detection for sandwich bond strength evaluation required another means of stressing the bondline. To achieve large bond stresses, a suction cup was fabricated with a springmounted ultrasonic transducer in its center, for use in a pressure chamber. With the inside of the vacuum cup vented to atmosphere, the force on the bond is equivalent to the pressure in the chamber. The transducer, installed within the vacuum cup, transmits the ultrasonic bond stress noise emissions to the equipment. The signals are monitored and the predicted bond failure point is judged by the operator. This type of testing is impractical for large sandwich structure evaluations. The same results may be obtained by edge-sealing of the structure and installation of removable pressure valves.

## ULTRASONIC EMISSION DETECTOR

The ultrasonic emission detection equipment constructed for this program may be applied as shown in Figure 4. A transducer or microphone capable of detecting or measuring ultrasonic vibrations is mounted on the metal surface of the test specimen in the vicinity of the bond. For a large complex structure, several transducers may be required. The transducer output is amplified and selectivity filtered so that only vibrations in a particular frequency band are passed on to the data translation system, which converts these signals to frequencies in the audio spectrum, permitting the signals from the specimen to be heard via a set

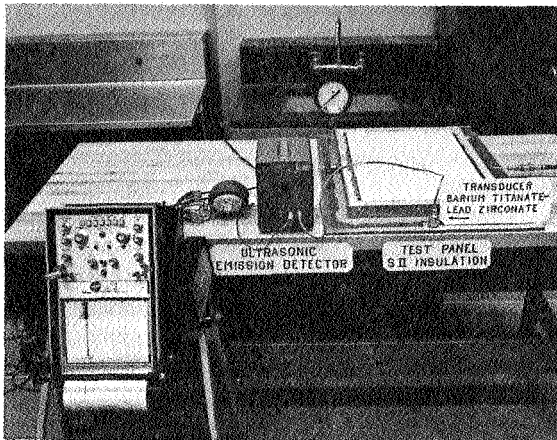


FIGURE 4. ULTRASONIC EMISSION DETECTOR APPARATUS

of earphones or a loudspeaker. The data can be suitably processed for display on an oscilloscope or a recorder through the accessory equipment outlet on the back of the chassis.

Figure 5 is a block diagram of this unit. The

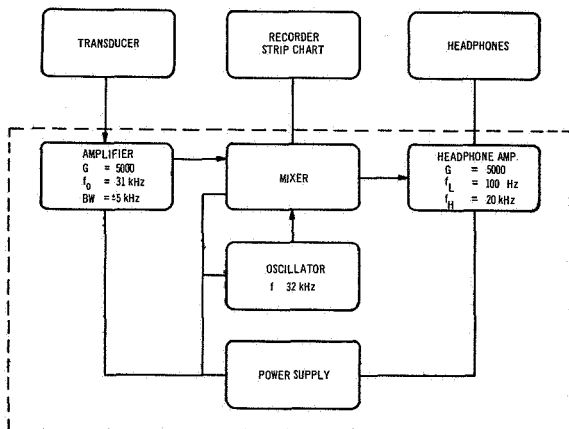


FIGURE 5. BLOCK DIAGRAM OF ULTRASONIC EMISSION DETECTOR

output of the transducer is amplified with a gain of 5000 and a restricted usable bandwidth of 5 kHz on either side of a 31 kHz center frequency. This

allows energy in a frequency band of 26 kHz through 36 kHz to be amplified and processed. The input of this amplifier can handle large signals below 26 kHz without distortion so that the noise pulses, either from the test fixture or a shop environment, which are below 26 kHz, are attenuated and do not disturb the system. The amplifier output and a signal from a 32 kHz oscillator are fed to a mixer. The mixer produces the sum and difference frequencies of the two inputs, although only the difference frequencies are used. These difference frequencies are in the audible range (approximately 0-6 kHz); therefore, one output of the mixer is connected to a set of headphones for use by the operator in monitoring the noise generated by the adhesive under stress. The other output of the mixer is used to drive a recorder, or other accessory; thus the data from this equipment can be interpreted while the sample or structure is being stressed.

Acoustical energy in the sonic and ultrasonic region is generated when stresses are applied to materials. This effect is presently being used by Delcon Corporation and Western Inspection Service to detect evidences of plastic deformation in metal structures, and by the Metals & Ceramics Division of Wright-Patterson in Dayton to determine how boron filaments break up.

Results indicate that adhesive ultrasonic emission above 16 kHz can be used to predict when a bond will fail. Acoustic emission also occurs at lower frequencies, however, considerable noise is generated below 16 kHz by the test fixture, as shown in Figure 6. For each of the adhesives tested, i.e., FM-1000, HT-424, and Metlbond 329, there is a large increase in noise above 16 kHz as the ultimate strength of the bond is approached. Thus, if a method of stressing a bond is available, this technique provides a means of determining bond strength.

The acoustical energy generated from sandwich or metal-to-metal bonded specimens under stress can easily be distinguished from the sounds of the test stand or environment. The adhesive produces many very short duration bursts of energy that sound like a high-pitched crackling noise. The amplitude of the emitted signals becomes significantly stronger as the yield stress is approached, and can be used to predict the yield point and ultimate strength without damage to the structure.

The test results presented in Table II for metal-to-metal bonds are for Metlbond 329 and HT-424 adhesives only. Strength limitations of the test

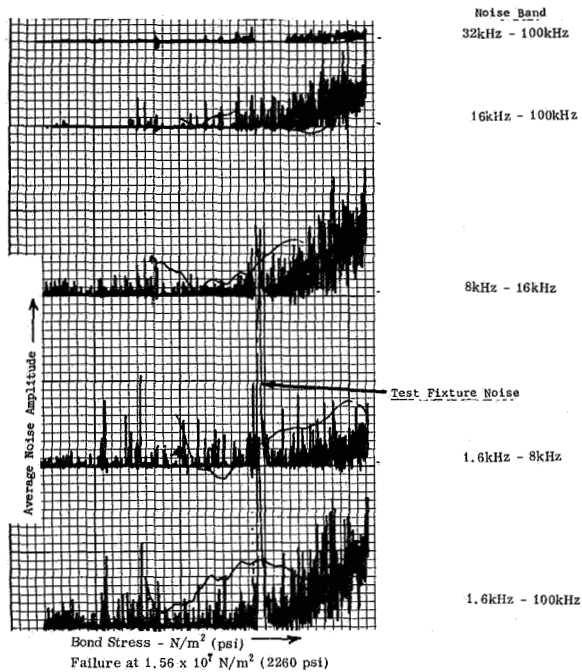


FIGURE 6. STRESS NOISE EMISSION SPECTRUM FOR HT-424 ADHESIVE IN FLATWISE TENSION AND 40% BONDLINE CONTAMINATION

fixture prevented evaluation of FM-1000. Other investigations of FM-1000 verify that it has similar acoustic emission response characteristics.

The prediction errors ranged from three to thirty percent, i. e., deviation of predicted breaking point from actual failure. This range is influenced by the evaluation of the ultrasonic emission method and the ultrasonic attenuation method at the same time on the same specimen. The predicted value of the breaking point was determined initially by stressing the sample at a constantly increasing rate to the maximum bond pressure determined by the operator. From this point upward to the actual failure point, the specimens were subjected to alternate tension - compression cycling from the dynamics required for the ultrasonic attenuation test. This varying stress rate influenced the point at which the actual breaking point occurred and thereby produced the large errors. The incorporation of an electronic gating circuit at the output of the detector would decrease the possibility of operator judgment error. The electronic gating circuit can be set to energize a warning lamp or buzzer when the amplitude of the average peak-to-peak noise level, as determined from previous destructive tests, reaches the point where ultimate strength may be predicted.

Methods employing internal pressure to stress the face sheets of sandwich panels having a perforated honeycomb core must consider the porosity of the adhesive if the integrity of the bond between the adhesive and the face sheet is to be verified. The thickness of the face sheet determines what portion of the force is absorbed in the face sheet and what portion of the force stresses the bond. With a thicker face sheet, the samples failed at a substantially higher value.

Testing sandwich panels with phenolic honeycomb core revealed that the phenolic core generates more ultrasonic energy than the adhesive. The phenolic core was not perforated to relieve internal pressure as was the aluminum honeycomb core, therefore, the high pressure vacuum cup and other internal stress induction methods could not be used. External compression or tension can be used to determine when core failure begins for unperforated phenolic core sandwich panels. Further evaluation of perforated non-metallic core sandwich structures is advised, based upon cryogenic insulation used on the S-II stage of the Saturn V vehicle.

Noise emission spectrum graphs supplied by the contractor were essentially the same for both perforated core or laminated types of bonded structures. Well bonded samples emitted little or no noise below ninety percent ultimate strength, while poorly bonded samples started emitting noise at lower levels, depending on the adhesive used. Further inhouse work on equipment applications will expand the prediction results based on structures and adhesive systems used in Saturn and subsequent programs.

The Ultrasonic Emission Detector is applicable, nondestructively, to metal bonded to metal, and metal bonded to non-metal in laminate and sandwich core structures. It is limited to some extent by configuration, materials, and stress induction methods. Some of the merits of this equipment are as follows: (1) Low bond strength can be detected. When concentrated stresses sufficient to cause limited failure occur in defective areas, the noise emission is large enough, in most adhesives, for determination of the ultimate bond strength or bond quality. The weaker the bond the more noise emitted for a given stress, as tiny areas fail in the weak bond locations. The total amount of noise emitted, may, therefore, be equated to an indication of bond quality. Some examples of the multitude of material and structural variations which affect bond strength and produce noise are voids and porosities, inadequate cleaning, debonded areas, residual stresses, and inadequate cure. (2) The equipment is

TABLE II. BOND STRENGTH PREDICTION RESULTS

ADHESIVE	CONTAMINATION	ESTIMATED 90% ULTIMATE STRENGTH	PREDICTED ULTIMATE STRENGTH	ACTUAL ULTIMATE STRENGTH	PERCENT DEVIATION OF PREDICTED BREAK- ING POINT FROM ACTU- AL BREAKING POINT
		N/m <sup>2</sup> × 10 <sup>7</sup> (psi)	N/m <sup>2</sup> × 10 <sup>7</sup> (psi)	N/m <sup>2</sup> × 10 <sup>7</sup> (psi)	
MB-329	NONE	1.72 (2500)	1.90 (2750)	2.58 (3750)	-27%
	20%	1.45 (2100)	1.60 (2310)	1.74 (2520)	- 8%
	20%	1.45 (2100)	1.60 (2310)	1.50 (2180*)	+ 6%
	30%	1.10 (1600)	1.21 (1760)	1.31 (1900*)	- 7%
	40%	0.965 (1400)	1.06 (1540)	1.03 (1500)	+ 3%
	40%	0.689 (1000)	0.758 (1100)	0.792 (1150)	- 4%
HT-424	NONE	4.00 (5800)	4.40 (6380)	3.72 (5400*)	+18%
	20%	2.45 (3550)	2.69 (3900)	2.20 (3200*)	+22%
	20%	1.50 (2180)	1.65 (2400)	1.43 (2075)	+16%
	40%	1.63 (2360)	1.79 (2600)	1.84 (2670*)	- 3%
	40%	2.55 (3700)	2.81 (4070)	2.15 (3120*)	+30%

\* ± 5% accuracy; all others ± 1%

- NOTES: 1. TESTS PERFORMED IN FLATWISE RING TENSION BETWEEN CYLINDRICAL BLOCKS. ONE BLOCK RECESSED TO FORM OUTER ANNULUS OF 32.2 cm<sup>2</sup> (5 in<sup>2</sup>) BOND AREA.
2. FIXTURE STRENGTH LIMITS PREVENTED FM-1000 TEST.
3. THE POINT FROM WHICH, BASED ON HEARING JUDGMENT, A 10% INCREASE WOULD FAIL THE TEST SAMPLE.
4. IN ALTERNATE TENSION-COMPRESSION CYCLING.

portable. (3) It is independent of configuration. The sound is transmitted along the face sheet material to the stationary transducer. Configuration size may influence sound level, but has not been evaluated as yet. (4) No liquid couplants are required. (5) The equipment is inexpensive at approximately one thousand dollars per unit, exclusive of accessory recording equipment which is in standard lab supply. (6) Large areas can be evaluated in one operation. Noise emitted by highly stressed areas is radiated in all directions through the face sheet to the stationary transducer or transducers. Maximum area of coverage by one transducer has not been determined. (7) Nominal skill is required to operate the equipment. (8) It can readily be adapted for automatic test evaluation. With attachment of an electronic gating circuit to the equipment output, a go-no-go system can be devised based on the level of noise

emission detected. Location of noise emitting areas can be established by three or more transducers and the use of triangulation techniques. Scanning of the structure is not required since the transducer or transducers are stationary. The bonded structures that are rejected can be tested with other types of equipment to determine the cause of excessive noise emission. (9) This equipment may be used on metal and non-metal composites if the transducer can be mounted on the bonded metal surface.

The limitations of the Ultrasonic Emission Detector equipment are as follows: (1) Surface contact is required. The transducer must be securely attached to the structure. (2) Structural bond-line stressing is required. (3) Density, material, and thickness combination affect the readout, as on all nondestructive test methods. The noise level

emitted by stressed structures will decrease with increased face sheet thickness and core density, for a given stress. Variation in metals will affect the readout because of their different densities. (4) The equipment does not define defects. Only noise signal levels, as emitted from areas of high stress concentration, are discerned and interpreted from noise level standards. (5) The basic equipment does not locate defects. An instrument with three channel capability and three transducers could be used with triangulation techniques and a real-time computer to locate defect areas. (6) Structural test specimen evaluation is required prior to equipment production applications. Noise level standards must be determined. Values must be established for panel reject/accept conditions based on noise emission ranges from satisfactory panels. (7) The transducer must be applied to a metal surface. Non-metallic surfaces rapidly attenuate the noise signals from distant areas. Further application studies will be made to determine exact distance limitations in all types of bonded structures and their component materials. (8) The basic equipment requires operator interpretation of audio signal intensity. The operator's sense of hearing may vary at times and produce inconsistent results. Minimum backup equipment for optimum evaluation would be an electronic gating circuit and a strip chart recorder. (9) Access to both sides of the test surface for transducer attachment may be required for a bonded honeycomb sandwich structure. No evaluations were performed on a sandwich structure to determine if the opposite side stress noise emission level was high enough to use only one transducer.

Specific areas where further development of this equipment is recommended for adhesion bond strength analysis are as follows: (1) Equipment may be used to obtain data on the dual-seal and the 4.06-centimeter (1.6-inch) foam and plastic laminate panels during proof-pressure tests of panel integrity on the S-II cryogenic insulation. (2) A check on each individual edge-sealed section of the instrument unit structure by pressurization may be performed. (3) Nondestructive and destructive test data may be obtained during the strength tests to be performed inhouse on the 3.05- and 6.60-meter (120- and 260-inch) diameter metal honeycomb sandwich shrouds. A check of each individual edge-sealed section by pressurization would be required. (4) Data may be obtained where the common bulkheads of the S-II and S-IV stages can be internally pressurized or externally stressed. It may also be possible to monitor bulkhead bondline noise emissions over periods of storage or installation time where built-in residual stresses may cause gradual

debonding. (5) Payload shrouds and nosecones may be evaluated by proof pressure or static loading. (6) Data may be obtained from structural destructive tests of any bonded structure bonded with the adhesives, or equivalent, evaluated by this program. Information from these tests indicates when the adhesive bonds start to yield, and gives the bondline stress noise emission characteristics from stress induction until complete structural failure. Yield point and allowable noise levels may then be established for the particular structure and used on future nondestructive test evaluations. (7) Structural static or dynamic load tests of bonded brackets or other bonded structural attachments will give information on the bond integrity. The possibility exists that a static test would start a bond failure, but failure would not occur in creep before completion of the test period. Noise emission from the bondline during static stress would indicate the quality of the bond.

In order to extend applications of the Ultrasonic Emission Detector, test programs are under way to establish the maximum evaluation range of the transducer and the effect of other adhesives, metals, and nonmetals that are used in bonded structures. Evaluation of defective bonds and associated noise emission characteristics will be undertaken.

## CONCLUSION

The contract with General American Transportation Corporation was completed on September 8, 1965, with a demonstration of ultrasonic emission detection equipment for adhesion bond strength determinations in stressed composite structures. For bondline strength control, the photomicroflaw method satisfied the need for simulation of poor bond strengths through controlled surface contamination.

Rigid cleaning, holding time limits, and handling requirements for cleaned parts prior to bonding, as contained in all satisfactory specifications and as required by military specification MIL-A-9067C, "Process and Inspection Requirements for Adhesive Bonding," were verified by this program [4].

The ultrasonic signal emissions from a stressed bondline, modulated for acoustic monitoring, were found to be a reliable indication of bond strength. Noise signal level increases with the amount of stress applied to the bondline. Weak bonds and

delaminated areas produced noise above established standard levels, thus indicating rejection of the defective panel. The Ultrasonic Emission Detector may be used to evaluate destructive tests on specimens and structures. Data obtained will indicate when the adhesive bond starts to yield and give the bondline stress noise emission characteristics from stress induction until complete structural failure, so that allowable noise level standards may

be established for nondestructive evaluation. Non-destructive evaluation may be made on structures containing perforated cores that can be edge-sealed and internally pressurized, and on structures where stresses can be induced externally by mechanical fasteners or fixtures. Brackets and associated attachments, bonded to structures, may also be evaluated and are one of the most immediate applications for this equipment.

## REFERENCES

1. Schmitz, Gerald; and Frank, Louis: Nondestructive Testing for Evaluation of Strength of Bonded Material. Contract NAS8-11456, General American Research Division, General American Transportation Corporation, Niles, Illinois, September 1966.
2. Military Specification MIL-A-005090E (Wep), Adhesives, Heat Resistant, Airframe Structural, Metal to Metal. April 22, 1963.
3. Military Specification MIL-A-25463 (ASG), Adhesive Metallic Structural Sandwich Construction. January 14, 1958.
4. Military Specification MIL-A-9067C, Adhesive Bonding, Process and Inspection Requirements for.

## BIBLIOGRAPHY

1. Braddock, P. H.: New Method for NDT Uses Ultrasonic Waves from Loads. Metalworking News, October 5, 1964.
2. Judge, John F.: Nondestructive Testing Fundamental to Advanced Materials Development. Missiles and Rockets Publication, February 22, 1965, pages 27-32.
3. New NDT Method Probe: The Look, Sound, and Smell of Quality. Steel, The Metalworking Weekly, February 14, 1966.
4. Schmitz, G. L.: Nondestructive Testing of Adhesive Bonds. Design News Publication, September 15, 1966, page 182-185.
5. Simpkins, Alan B.: Silent Sounds of Industry. Design News Publication, March 16, 1966, pages 50-53.